J Neural Transm (2007) 114: 693–698
DOI 10.1007/s00702-007-0670-3
Printed in the Netherlands

Journal of Neural Transmission

The aromatic cage in the active site of monoamine oxidase B: effect on the structural and electronic properties of bound benzylamine and *p*-nitrobenzylamine

M. A. Akyüz[1], **S. S. Erdem**[1], **D. E. Edmondson**[2]

[1] Department of Chemistry, Faculty of Arts and Sciences, Marmara University, Göztepe, Istanbul, Turkey
[2] Departments of Biochemistry and Chemistry, Emory University, Atlanta, Georgia, U.S.A

Received: October 13, 2006 / Accepted: November 22, 2006 / Published online: March 31, 2007

Summary Computational studies using the ONIOM methods have been performed to probe the catalytic roles of tyrosine residues 398 and 435 which constitute the "aromatic cage" in the active site of MAO-B. The results presented here provide additional new insights into the interactions that take place on activation of the amine substrate by the aromatic cage residues in MAO-B catalysis and have relevance to the MAO-A catalytic mechanism.

Keywords: ONIOM calculations, neurotransmitter, FAD binding site, enzyme modeling

Introduction

With the elucidation of the detailed structures of MAO-A (Ma et al., 2004; Colibus et al., 2005) and of MAO-B (Binda et al., 2002, 2003, 2004), the detailed active site structures have resulted in new insights into possible mechanisms of catalysis. In both enzymes, the *re* face of the covalent flavin coenzyme faces the substrate binding site and two tyrosyl residues are situated 7.8 Å apart in an approximately parallel configuration such that the amine substrate must pass between the two phenolic rings to reach the flavin for catalysis. This type of structure is observed in other flavin-dependent amine oxidizing enzymes (Trickey et al., 2000; Binda et al., 1999) and appears to have functional significance. Recent kinetic and structural studies by Li et al. (2006) on Y435 mutants of MAO-B suggest the functional role of this aromatic cage involves both steric and dipole coupling effects to activate the amine substrate by enhancing its nucleophilicity for attack on the flavin coenzyme as illustrated in the model shown in Fig. 1. These results have been suggested as providing further support for the polar nucleophilic mechanism of amine oxidation (Miller and Edmondson, 1999) in which amine oxidation is initiated by the nucleophilic attack of amine nitrogen on the flavin with the N(5) of the C(4a) adduct abstracting the α-carbon proton of the amine. Our recent computational study also supports this mechanism (Erdem et al., 2006).

To provide further insights into these proposed roles suggested for the aromatic cage in amine oxidation as well as to provide information that is not readily accessible by experimental techniques, we have initiated computational studies to investigate the molecular events involved. Alterations in the structural and electronic properties of the substrates have been investigated as they travel through the aromatic cage at the active site of MAO-B.

Correspondence: Safiye Sag Erdem, Chemistry Department, Faculty of Arts and Sciences, Marmara University, Göztepe, 34722 Istanbul, Turkey
e-mail: erdem@marmara.edu.tr

Materials and methods

Various computational methods have strengths and weaknesses. Quantum mechanics is able to compute electronic properties and model chemical reactions. However, the accurate *ab initio* modeling of chemical systems containing a large number of atoms is still a challenging task. An obvious solution to this problem is the partitioning of the system into two or more parts or layers using a QM/MM approach. The crucial part of the system (the inner layer) is treated at a high level of theory using quantum mechanics. The rest of the system (outer layer) is described by a computationally less demanding molecular mechanics method. An alternative formulation of QM/MM is the so called "ONIOM" method introduced by Morokuma and co-workers (Dapprich et al., 1999). In this method, calculations are

done on various regions of the molecule with various levels of theory. Then the energies are added and subtracted, to give suitable corrections. ONIOM method has been proven to be very valuable for treatment of large molecular systems like enzymes. In this work, three layer ONIOM calculations were applied to the FAD binding site of MAO-B.

Benzylamine and *p*-nitrobenzylamine were used as substrates in the calculations. The amino group lies perpendicular to the benzene ring in the most stable conformations of benzylamine and *p*-nitrobenzylamine in their isolated forms. However, in the X-ray structure of *p*-nitrobenzylamine complex with human MAO-B, the amine N lies on the same plane of the benzene ring which is oriented approximately parallel to the phenolic rings of Y435 and Y398 (Li et al., 2006). Therefore, we have investigated the behaviour of both perpendicular and planar conformations for these two substrates.

The 2.2 Å crystal structure of human MAO-B in complex with deprenyl was obtained from protein data bank (2BYB) with the FAD and substrate binding site structures used in the calculations. Deprenyl was deleted from the structure and isoalloxazine ring of FAD was optimized to its oxidized form with semiempirical PM3 method; freezing the coordinates of the remaining atoms. The substrates were then inserted in the active site. ONIOM (HF/6-31G*:PM3:UFF) calculations were performed with Gaussian 03 (Frisch et al., 2004). The substrate was selected as the inner (high) layer and optimized at the *ab initio* HF/6-31G* level. Flavin, tyr435, tyr398, cys172, gln206, phe343, tyr326, leu171, and ile199 (partially) were selected as the medium layer and semi empirical PM3 calculations were applied. Other important active site residues (tyr60, tyr188, ile198, leu328, thr399, gly434) were treated as the outer (low) layer using molecular mechanics UFF method. The geometrical parameters of all heavy atoms in the medium and low layers were frozen prior to calculation. Selected distances between the substrate benzyl carbon and flavin N(5) were constrained to ten different values ranging from 2 to 6 Å and the energy of the system described above was calculated at each constrained point. Energy profiles with respect to the constrained distances were obtained. At the minimum energy points of these profiles, the substrates were fully optimized; freezing the parameters of other active site heavy atoms. Thus, the most stable positions of the substrates at the active site were determined. In order to investigate the electronic charges, structures obtained from ONIOM calculations of each constrained distance were subjected to single point HF/6-31G* calculations for the overall system used. Therefore, all the data related to electronic Mulliken charges were obtained at the HF/6-31G* level.

After the substrate enters the active site it is assumed to travel towards the flavin between the aromatic tyrosine residues (Y435 and Y398). Thus, the partial electronic charges on the amine group can be influenced by both the flavin and the tyrosine rings. To observe the influence of flavin ring, a smaller model system was generated, by preserving only the flavin and substrate portion of the overall structure obtained from ONIOM calculation; all the remaining active site groups were erased. This procedure was repeated for each constrained distance between the substrate benzyl carbon and flavin N(5). Then, single point HF/6-31G* calculations were applied at each constrained distance. In order to eliminate the influence of the flavin on the electronic charge of a certain atom in the substrate, the following equation was used:

$$\text{Net aromatic cage effect on charge} = |\text{Charge in overall structure} - \text{Charge in model system}|$$

Results

Energy profiles

Energy profiles with respect to the constrained distances between benzyl α-C and flavin N(5) are given in Fig. 2 for two different conformations of each substrate. In the perpendicular conformations, the benzene ring moiety is oriented slightly below the aromatic cage and approximately perpendicular to the tyr435 and tyr398 as shown

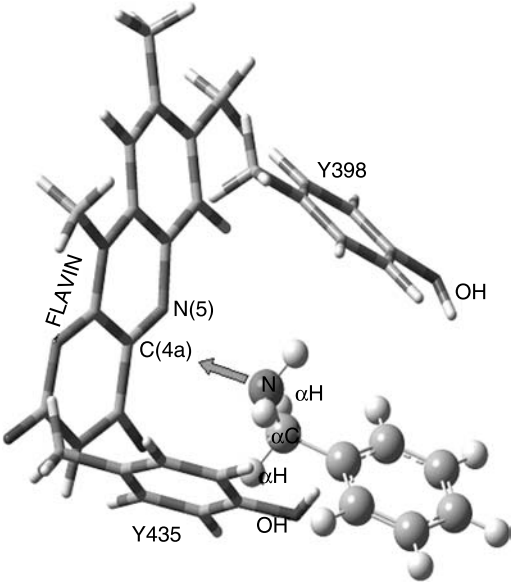

Fig. 1. Aromatic cage in the active site of human MAO-B in complex with perpendicular benzylamine. The lone pair electrons of benzylamine nitrogen are directed to the C(4a) of flavin for nucleophilic attack. Other active site residues included in calculations are not shown for clarity

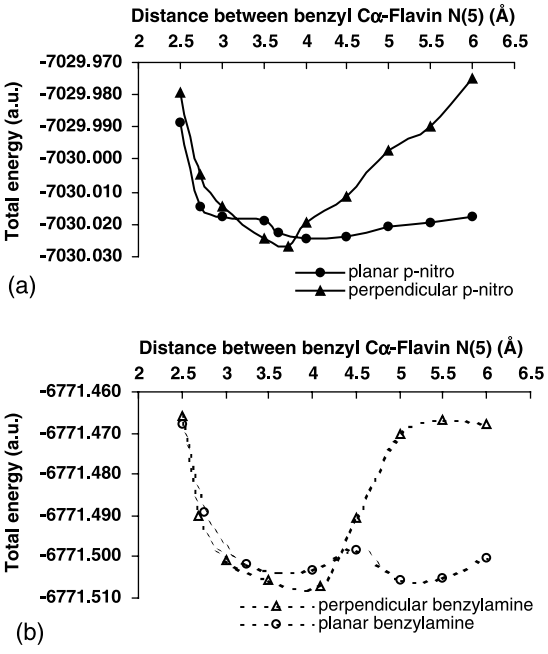

Fig. 2. Energy profiles of (**a**) *p*-nitrobenzylamine (**b**) benzylamine at the active site obtained from single point HF/6-31G* calculations using the optimized geometries obtained from ONIOM (HF/6-31G*:PM3:UFF) method

in Fig. 1 whereas in the planar conformation, it is parallel to these tyrosyl residues. Figure 2 demonstrates that the aromatic cage does not alter considerably the energy of the substrate in planar benzylamine orientations. However, the energies of the perpendicular substrates decrease steadily as they travel into the active site up to a minimum value at about 3.5–4 Å, which corresponds approximately to the center of the aromatic cage. Meanwhile, the orientation of the benzenoid ring deviates from its perpendicular conformation (data not shown) and adopts a "near attack conformation" when it is in close proximity to the flavin. Although the perpendicular conformation has been found to be slightly more stable for the isolated substrates, the planar conformation is much more stable in the active site of MAO-B when the substrates are 4–6 Å from the flavin. The results described above are similar for both substrates with the exception that hydrogen bonding interactions of the nitro oxygens of *p*-nitrobenzylamine with the thiol hydrogen of cys172 occurs as will be discussed in detail in the discussion section. For perpendicular *p*-nitrobenzylamine, these interactions have been observed when the distance between α-C and N(5) is shorter than 4.5 Å. However, in planar *p*-nitrobenzylamine, they exist at every computed distance between 6–2.75 Å and become much stronger at distances shorter than 4.5 Å. The hydrogen bonding interactions between nitro and thiol groups no longer exist when the distance between α-C and N(5) is shorter than 2.75 Å, for either conformation.

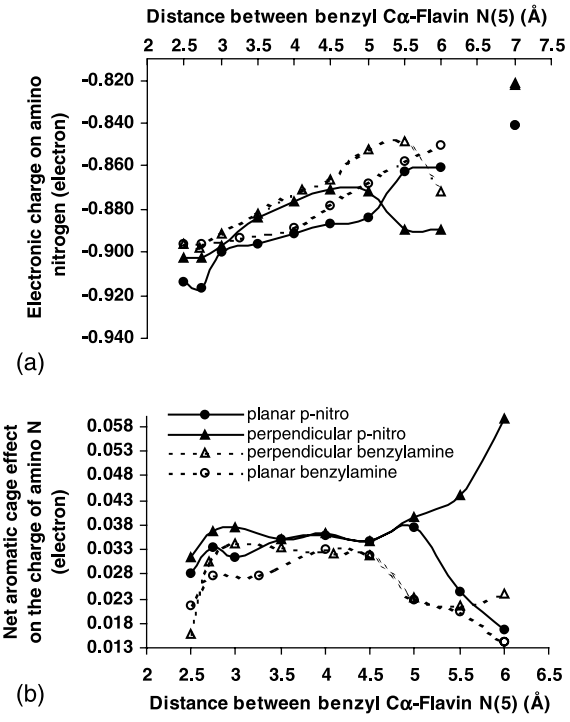

Fig. 3. (**a**) Electronic charge profile of the substrate amine nitrogen at the active site. The points outside the plot are the electronic charges on the free substrates. (**b**) Net aromatic cage effect on the electronic charge of amine nitrogen

Electronic charge profiles

Alterations in electron densities of the relevant atoms with respect to the constrained distances of substrate Cα to flavin N(5) (from 2 to 6 Å) were investigated. Data at 2 Å were omitted from the plots because the structures became somewhat distorted due to their proximity to the flavin.

Variations in negative charge of the amine nitrogen with respect to the distance between flavin and the substrates is shown in Fig. 3a. For the purpose of comparison, the charges of the isolated structures were also given in the same plot. There is an apparent enhancement in the negative charge on nitrogen for each substrate when it is inserted into the active site. Some irregularities are observed at distances 5–6 Å as discussed below. At distances closer than about 5 Å, the magnitude of negative charge increases steadily as the substrate approaches the flavin. It seems that flavin also increases the charge density on the amine nitrogen as the substrate becomes closer to it. In order to obtain the net active site effect, the influence of flavin was excluded as described in methodology. The data was shown in Fig. 3b. Values on the vertical axis represent the change in magnitude of negative charge on amine nitrogen. As expected, the portion of the graph between 4.5 and 2.75 Å exhibits nearly constant values because this interval corresponds to the path in aromatic cage without the influence of flavin. Outside this path, the effect declines rapidly, except for the case observed at longer distances as discussed below.

For benzylamine, the influence of the aromatic tyrosine residues can be observed in the 3–4.5 Å interval in which the electron density on the amine nitrogen increases considerably relative to the rest of the graph. In perpendicular benzylamine, hydrogen bonding interactions at the protein backbone slightly influence the charge on amine nitrogen at 6 Å, as the perpendicular conformation is distorted to interact with the oxygen of gln206 through the amine hydrogens. For planar *p*-nitrobenzylamine, the influence of the aromatic tyrosines initiates at 5 Å and continues until 2.75 Å. At 5 Å, its amine group does not actually enter the aromatic cage but exhibits hydrogen bonding interactions with the oxygen of tyr435. This interaction results in a decrease in the electron density of amine hydrogen interacting with the oxygen of tyr435 and an increase in the charge on the amine nitrogen. A similar interaction is present in the perpendicular *p*-nitrobenzylamine conformation

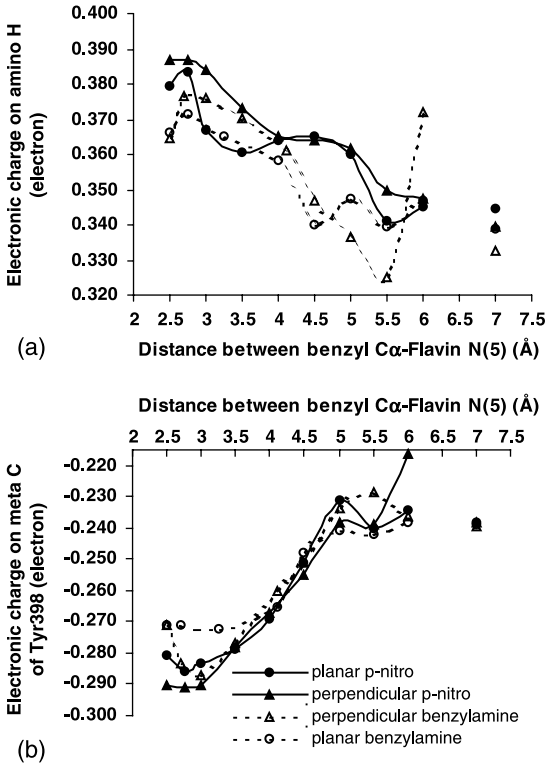

Fig. 4. Electronic charge profile of (**a**) hydrogen of amino group (**b**) carbon atom at the meta position of tyr398. The points outside the plot are the electronic charges on the free substrates for (**a**) and the free enzyme (**b**)

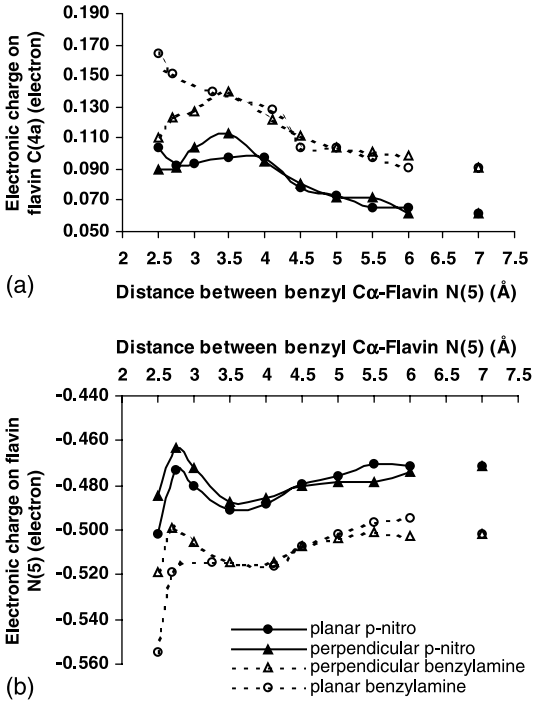

Fig. 5. Electronic charge profile of (**a**) C(4a) (**b**) N(5) of flavin ring. The points outside the plot are the electronic charges on the flavin of the free enzyme

both at 5 Å and at 6 Å. Therefore, charge enhancements observed at 5 Å and at 6 Å are due to the intermolecular hydrogen bonding interactions with tyr435. In addition, at 5.5 Å, the amine group changes its conformation from a perpendicular to a planar form and the amine hydrogens interact with electron density on tyr398. Therefore, perpendicular *p*-nitrobenzylamine shows some irregularities in the range 5–6 Å. Perpendicular benzylamine does not exhibit such interactions because it approaches the aromatic cage slightly below the path that *p*-nitrobenzylamine enters.

As the substrate approaches closer to the flavin, partial positive charge of the amine hydrogens increases (Fig. 4a), parallel to an increase in the partial negative charge of the amino nitrogen. A few anomalous points observed in these plots are due to the intermolecular interactions discussed above. At distances closer than about 3.5 Å, the partial positive charge on α hydrogen H(t) starts to increase rapidly, making it more and more acidic(data not shown). These changes influence the electron distribution in the flavin ring such that, around 3.5–4 Å, a positive charge on C(4a) and a negative charge on N(5) reach their peak values as shown in Fig. 5. This effect is more pronounced for the perpendicular conformations of these substrates. These events support the proposals that the Cα pro-R H is transferred to the flavin as a proton.

Another important feature is that, in comparison to free substrate structures, amino group nitrogens in the bound substrates exhibit larger negative charges (Fig. 3a) and amino hydrogens positioned between the aromatic tyrosyl rings exhibit larger positive charges (Fig. 4a). In this connection, complementary alterations in electron densities of tyrosyl carbons are observed relative to the free enzyme. Figure 4b shows that after the substrate amine group enters the aromatic cage, the negative charge on tyrosyl aromatic carbons (for example, the *meta* C position) of tyr398 increases as it approaches the flavin. Such changes are more apparent in tyr398 rather than in tyr435, because tyr398 is situated slightly lower than tyr435 and therefore the substrate travels through the aromatic cage in closer proximity to tyr398.

Discussion

Calculated geometrical parameters of optimized *p*-nitrobenzylamine complex in its planar conformation showed good agreement with its X-ray structural data (Li et al., 2006), indicating the quality of the calculations. These calculations were able to reproduce the intermolecular

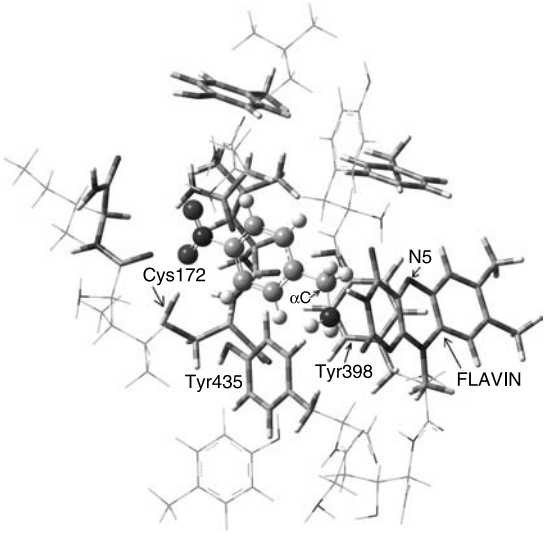

Fig. 6. Fully optimized structure of planar *p*-nitrobenzylamine complex of human MAO-B. Benzyl Cα–N(5) distance is 3.7 Å. ONIOM layers: High layer: *p*-Nitrobenzylamine, shown as ball and spoke model. Medium layer: Flavin, tyrosines and other residues, shown as tube model. Low layer: Atoms shown as wire model

H-bonding between the nitro oxygen and the hydrogen of cysteine 172 (Fig. 6). The distance between the oxygen atom of nitro group and the sulfur atom of cysteine was calculated to be 3.2 Å which is only 0.1 Å longer than the X-ray data. This H-bonding has been suggested to be responsible for the lower activity of *p*-nitrobenzylamine in comparison to benzylamine for MAO-B because such interactions retard the ability of the amine moiety to form productive complexes with the flavin for efficient catalysis.

The results explained in previous section suggest that an appropriate enzyme-substrate complex forms around 3.5–4 Å, then the reaction starts and approaches the transition state at about 2.75–2.5 Å (corresponds to 2.99–2.87 Å for N_{amino}–C(4a) distance). Meanwhile, a more stable perpendicular conformation of amine moiety becomes more and more distorted and approaches an approximately planar conformation with respect to the benzene ring. For example, as benzylamine approaches the flavin at 5.5, 4.5, 3.5, and 2.5 Å, the N_{amino}–C_α–C–C dihedral angle decreases, respectively as follows: 89, 73, 60, 23°. It seems that the substrate approaches a more ''near attack conformation'' (NAC) required for the nucleophilic attack of the amine nitrogen on the C(4a) of the flavin and it reaches the transition state around 23° and is expected to lose its α proton. These structural and electronic features are consistent with the previous gas phase computational study at the B3LYP/6-31G* level (Erdem et al., 2006). For instance, in the gas phase transition state structure, the same dihedral angle was found to be 24°; Cα–N(5) and N_{amino}–C(4a) distances were predicted to be 2.96 and 2.80 Å, respectively. On the other hand, according to the present ONIOM study, the perpendicular conformation of *p*-nitrobenzylamine is less distorted relative to benzylamine. The same dihedral angle diminishes to only 55° at 2.5 Å. We suggest that the H-bonding between the nitro group and the cys172 retards the rotation of the benzene ring and thus prevents it from adopting a perfect NAC conformation, which may be responsible for the lower activity measured for *p*-nitrobenzylamine.

Figure 2 indicates that the most stable position of each substrate at the active site corresponds to the center of the aromatic cage. Alterations in the energy profile together with the observed deviations from perpendicular conformations inside the aromatic cage implies that aromatic cage facilitates the formation of a stable pre-reactive enzyme-substrate complex providing the necessary energetic and conformational changes.

In addition, except for a few anomalous points at longer distances, the negative charge on the amine nitrogen exhibits larger values along the path in the aromatic cage until the substrate reacts with flavin at about 2.75 Å (Fig. 3). This result and other electronic features in Figs. 4 and 5 suggest that the function of the aromatic cage is to increase the nucleophilicity of the amine substrate by re-distributing the electron density to achieve electrostatic complementarity between partial charges of the tyrosines and the amino group. Similar calculations on Y435 mutant proteins are in progress to investigate the relationship between mutant activities and charge distribution.

Acknowledgement

This work was supported by the Marmara University Scientific Research Projects Commission (BAPKO), project no: FEN-YYP-290506-0141. DEE acknowledges support from the National Institutes of Health (GM29433). We are grateful to Prof. K. Yelekçi for invaluable discussions.

References

Binda C, Coda A, Angelini R, Federico R, Ascenzi P, Mattevi A (1999) A 30-angstrom-long U-shaped catalytic tunnel in the crystal structure of polyamine oxidase. Structure 7: 265–276

Binda C, Newton-Vinson P, Hubalek F, Edmondson DE, Mattevi A (2002) Structure of human monoamine oxidase B, a drug target for the treatment of neurological disorders. Nat Struct Biol 9: 22–26

Binda C, Li M, Hubalek F, Restelli N, Edmondson DE, Mattevi A (2003) Insights into the mode of inhibition of human mitochondrial monoamine oxidase B from high-resolution crystal structures. Proc Natl Acad Sci USA 100: 9750–9755

Binda C, Hubalek F, Li M, Herzig Y, Sterling J, Edmondson DE, Mattevi A (2004) Crystal structures of monoamine oxidase B in complex with

four inhibitors of the N-propargylaminoindan class. J Med Chem 47: 1767–1774

Colibus LD, Li M, Binda C, Lustig A, Edmondson DE, Mattevi A (2005) Three-dimensional structure of human monoamine oxidase A (MAO A): Relation to the structures of rat MAO A and human MAO B. Proc Natl Acad Sci USA 102: 12684–12689

Dapprich S, Komaromi I, Byun KS, Morokuma K, Frisch MJ (1999) A new ONIOM implementation in Gaussian98. Part I. The calculation of energies, gradients, vibrational frequencies and electric field derivatives. J Mol Struct (Theochem) 461–462: 1–21

Erdem SS, Karahan Ö, Yıldız İ, Yelekçi K (2006) A computational study on the amine-oxidation mechanism of monoamine oxidase: Insight into the polar nucleophilic mechanism. Org Biomol Chem 4: 646–658

Frisch MJ, Trucks GW, Schlegel HB, Scuseria GE, Robb MA, Cheeseman JR, Montgomery JA, Vreven T, Kudin KN, Burant JC, Millam JM, Iyengar SS, Tomasi J, Barone V, Mennucci B, Cossi M, Scalmani G, Rega N, Petersson GA, Nakatsuji H, Hada M, Ehara M, Toyota K, Fukuda R, Hasegawa J, Ishida M, Nakajima T, Honda Y, Kitao O, Nakai H, Klene M, Li X, Knox JE, Hratchian HP, Cross JB, Bakken Adamo VC, Jaramillo J, Gomperts R, Stratmann RE, Yazyev O, Austin AJ, Cammi R, Pomelli C, Ochterski JW, Ayala PY, Morokuma K, Voth GA, Salvador P, Dannenberg JJ, Zakrzewski VG, Dapprich S, Daniels AD, Strain MC, Farkas O, Malick DK, Rabuck AD, Raghavachari K, Foresman JB, Ortiz JV, Cui Q, Baboul AG, Clifford S, Cioslowski J, Stefanov BB, Liu G, Liashenko A, Piskorz P, Komaromi I, Martin RL, Fox DJ, Keith T, Al-Laham MA, Peng CY, Nanayakkara A, Challacombe M, Gill PMW, Johnson B, Chen W, Wong MW, Gonzalez C, Pople JA (2004) Gaussian 03, Revision C.02. Gaussian, Inc., Wallingford CT

Li M, Binda C, Mattevi A, Edmondson DE (2006) Functional role of the ''aromatic cage'' in human monoamine oxidase B: Structures and catalytic properties of Tyr435 mutant proteins. Biochemistry 45: 4775–4784

Ma J, Yoshimura M, Yamashita E, Nakagawa A, Ito A, Tsukihara T (2004) Structure of rat monoamine oxidase A and its specific recognitions for substrates and inhibitors. J Mol Biol 338: 103–114

Miller JR, Edmondson DE (1999) Structure-activity relationships in the oxidation of para-substituted benzylamine analogues by recombinant human liver monoamine oxidase A. Biochemistry 38: 13670–13683

Trickey P, Basran J, Lian LY, Chen Z, Barton JD, Sutcliffe MJ, Scrutton NS, Mathews FS (2000) Structural and biochemical characterization of recombinant wild type and a C30A mutant of trimethylamine dehydrogenase from *Methylophilus methylotrophus* (sp. W(3)A(1)). Biochemistry 39: 7678–7688